A New Algorithm for Retrieving Aerosol Optical Thickness Using TERRA/MODIS Satellite Images

Man Sing Wong[1], Janet Nichol[2], Kwon Ho Lee[3], Zhanqing Li[3]

[1]Department of Land Surveying and Geo-Informatics, The Hong Kong Polytechnic University, Hong Kong
E-mail: m.wong06@fulbrightmail.org, wongmansing.charles@gmail.com
[2]Department of Land Surveying and Geo-Informatics, The Hong Kong Polytechnic University, Hong Kong
E-mail: lsjanet@inet.polyu.edu.hk, lsjanet@polyu.edu.hk
[3]Earth System Science Interdisciplinary Center, University of Maryland (UMD), USA

Abstract
Aerosol detection and monitoring from satellite platforms has made significant advances over the past decade. While several state-of-the-art aerosol retrieval techniques provide aerosol properties at global scale, the more detailed spatial patterns remain unknown because most of the relevant satellite sensors operate at coarse resolution. A new aerosol retrieval algorithm for the Moderate Resolution Imaging Spectroradiometer (MODIS) 500m resolution data has been developed to retrieve aerosol properties over land, which helps to address the aerosol climatic issues at local and urban scales. The results show that 500m Aerosol Optical Thickness (AOT) data from MODIS are highly correlated ($r = 0.94$) with AERONET sunphotometer observations in Hong Kong. This study demonstrates the feasibility of aerosol retrieval at "fine" resolution in urban areas, which can assist in studies of aerosol loading distribution and the location of pollution source areas.
Keywords
aerosol optical thickness, look-up-table, MODIS, surface reflectance

I. INTRODUCTION

Aerosol retrieval from satellite remotely sensed images basically aims to separate the aerosols by decomposing the Top-Of-Atmosphere(TOA) reflectance from surface reflectance and the Rayleigh path reflectance. This is complex because the surface reflectance from the ground is usually greater. The estimation of surface reflectance is therefore the key factor.

Kaufman and Tanré (1998) first proposed the Dense Dark Vegetation (DDV) method using a multi-wavelength algorithm with MODerate resolution Imaging Spectroradiometer (MODIS) satellite images. The DDV (known as collection 4) algorithm works only on vegetated areas with coverage larger than 60% where the surface reflectances are very low. This prohibits the use of aerosol estimation on areas of bright surface, such as deserts and urban areas. Chu et al. (2002) revealed that the MODIS collection 4 algorithm has a positive bias in comparison to the AErosol RObotic NETwork (Holben et al., 1998) sunphotometer data. Remer et al. (2005) and Levy et al. (2004) reported certain inherent problems in determining surface reflectance using the DDV algorithm. These results imply that inaccurate surface properties can lead to errors in aerosol retrieval. Recently, Levy et al. (2007) modified the surface reflectance determination in MODIS aerosol retrieval algorithm (known as collection 5) based on vegetation index ($NDVI_{SWIR}$) and the scattering angle. Although significant improvements of MOD04 collection 5 algorithm was shown both in the accuracy and spatial continuity of aerosol retrieval (Li, et al., 2007; Mi, et al., 2007), the southern China especially in Hong Kong and the Pearl River Delta (PRD) region has been identified as having a large error of AOT (Kaufman and Tanré, 1998). Li et al. (2007) found correlations of 0.66 and 0.84 for collection 4 and collection 5 data respectively compared with "insitu" hazemeter measurements in China, but there are still two major limitations of MOD04 data for local/urban scale studies, namely bright surfaces and spatial resolution. To overcome these limitations, new techniques are developed in this study.

Aerosol retrieval over bright surfaces is challenging because the land surfaces and aerosol content are not easy to differentiate due to the high reflectance values of both. Hsu et al. (2004, 2006) recently developed a Deep Blue algorithm for aerosol retrieval over desert, arid, semiarid and urban areas using MODIS images. This algorithm made use of the blue wavelengths where the surface reflectances are bright in red region and darker in blue region.

In this study, in order to obtain the surface information, a surface reflectance database was developed based on the minimum reflectance technique (MRT) (Herman and Celarier, 1997; Koelemeijer, et al., 2003). The accuracy was validated from the MODIS surface reflectance products (MOD09).

The coarse spatial resolution of the MODIS products (10 km) only provides meaningful depictions on a broad regional scale, whereas aerosol monitoring over complex regions, such as urban areas in Hong Kong (1095 km^2) (Figure 1) requires more spatial details. Li et al. (2005) have developed a 1km AOT algorithm based on the MODIS collection 4 algorithm for a

1082-4006/08/14(02)-86$5.00

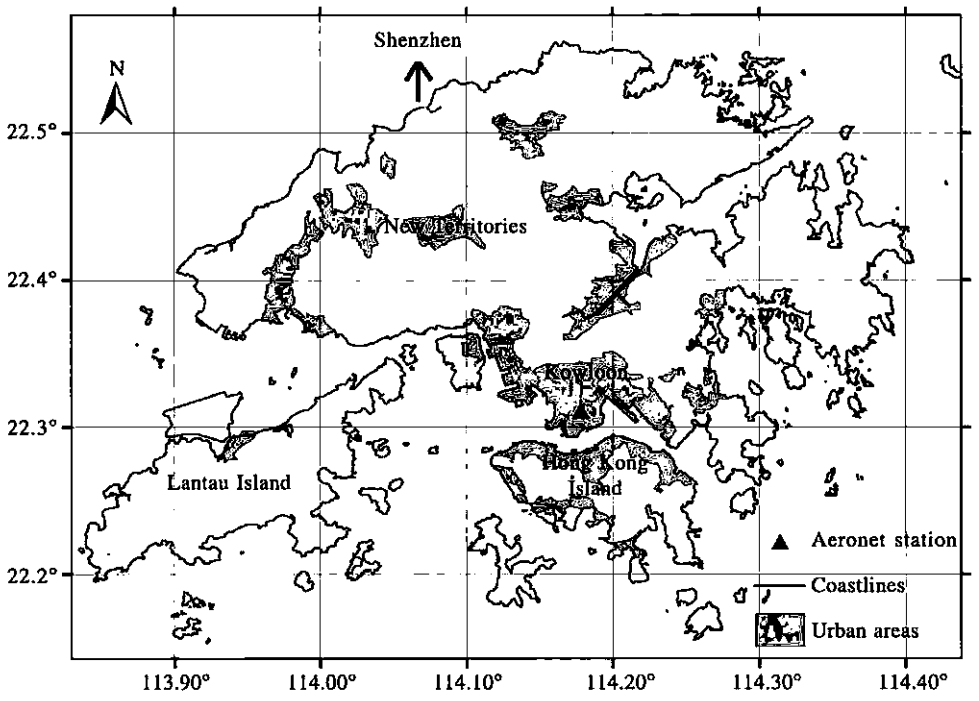

Figure 1. Map of Hong Kong and AERONET station

study in Hong Kong, but it was limited to dense vegetated areas and the results cannot be applied to urban areas. In order to retrieve the aerosol and map the aerosol loading distribution at detailed level, a new MODIS 500m resolution aerosol retrieval algorithm coupled with the modified MRT is presented in this study.

II. DATA USED

In this study, the 500m resolution TERRA/MODIS level 1B calibrated reflectance (MOD02HKM) and MODIS level 2 aerosol products (MOD04) of 2007 were collected. Validation of retrieved AOT was carried out by comparison with the AERONET data in Hong Kong. AERONET is a federated network of ground sunphotometers, which consists of a Cimel sunphotometer for measuring the aerosol extinction every fifteen minutes using a multiple wavelength radiometer.

III. METHODOLOGY

The rationale of the proposed aerosol retrieval algorithm is the determination of the aerosol reflectances by decomposing the Top-of-Atmosphere (TOA) reflectances from surface reflectance and the Rayleigh path radiance. The TOA reflectance $\rho_{TOA}(\theta_0,\theta_s,\phi)$is expressed as:

$$\rho_{TOA}(\theta_0,\theta_s,\phi)=\rho_{ATM}(\theta_0,\theta_s,\phi,\tau_{Aer},\tau_{Ray},p(\theta),\omega_0)+\frac{T_{Tot}(\theta_0)\cdot T_{Tot}(\theta_s)\cdot\rho_{Surf}(\theta_0,\theta_s)}{1-\rho_{Surf}(\theta_0,\theta_s)\cdot r_{Hem}(\tau_{Tot},g)} \quad (1)$$

where θ_0 is the solar zenith angle, θ_s is the satellite zenith angle, ϕ is the azimuth angle, τ_{Aer}, τ_{Ray} and τ_{Tot} are aerosol optical thickness, Rayleigh optical thickness, and total optical thickness respectively. $p(\theta)$ is the phase function, ω_0 is a single-scattering albedo, g is the asymmetry parameter, ρ_{ATM} is the atmospheric path reflectance, $T_{Tot}(m_0)$ is the total transmittance, $\rho_{Surf}(\theta_0,\theta_s)$ is the surface reflectance, and $r_{Hem}(\tau_{Tot}, g)$ is the hemispheric reflectance. Figure 2 illustrates the work flows of aerosol retrieval in this study. The discussion of Rayleigh path radiance, surface reflectances and Look Up Table (LUT) are illustrated in following sections.

A. Rayleigh and surface reflectances

The determination of the Rayleigh path radiance is based on the computation of spectral dependence of the Rayleigh optical depth and phase function. The equation 2 is adopted for calculating the Rayleigh scattering optical thickness (Bucholtz, 1995).

$$\tau_{Ray}(\lambda)=A\cdot\lambda^{-(B+C\lambda+D/\lambda)}\cdot\frac{p(z)}{p_0} \quad (2)$$

where A, B, C, D are the constants of the total Rayleigh scattering cross-section and the total Rayleigh volume scattering coefficient at standard atmospheres. $p(z)$ is the pressure relevant to the height and it is determined by a parameterized barometric equation (equation 3).

$$p(z)=p_0\cdot\exp\left[\frac{-29.87\cdot g\cdot 0.75\cdot z}{8.315\cdot(T_{Surf}-g\cdot 0.75\cdot z)}\right] \quad (3)$$

where g is the gravity acceleration (9.807ms^{-2}), T_{Surf} is the surface temperature(298K) (from the Hong Kong Observatory), and p_0 is the actual pressure in mean sea level (1008 Pa) and z

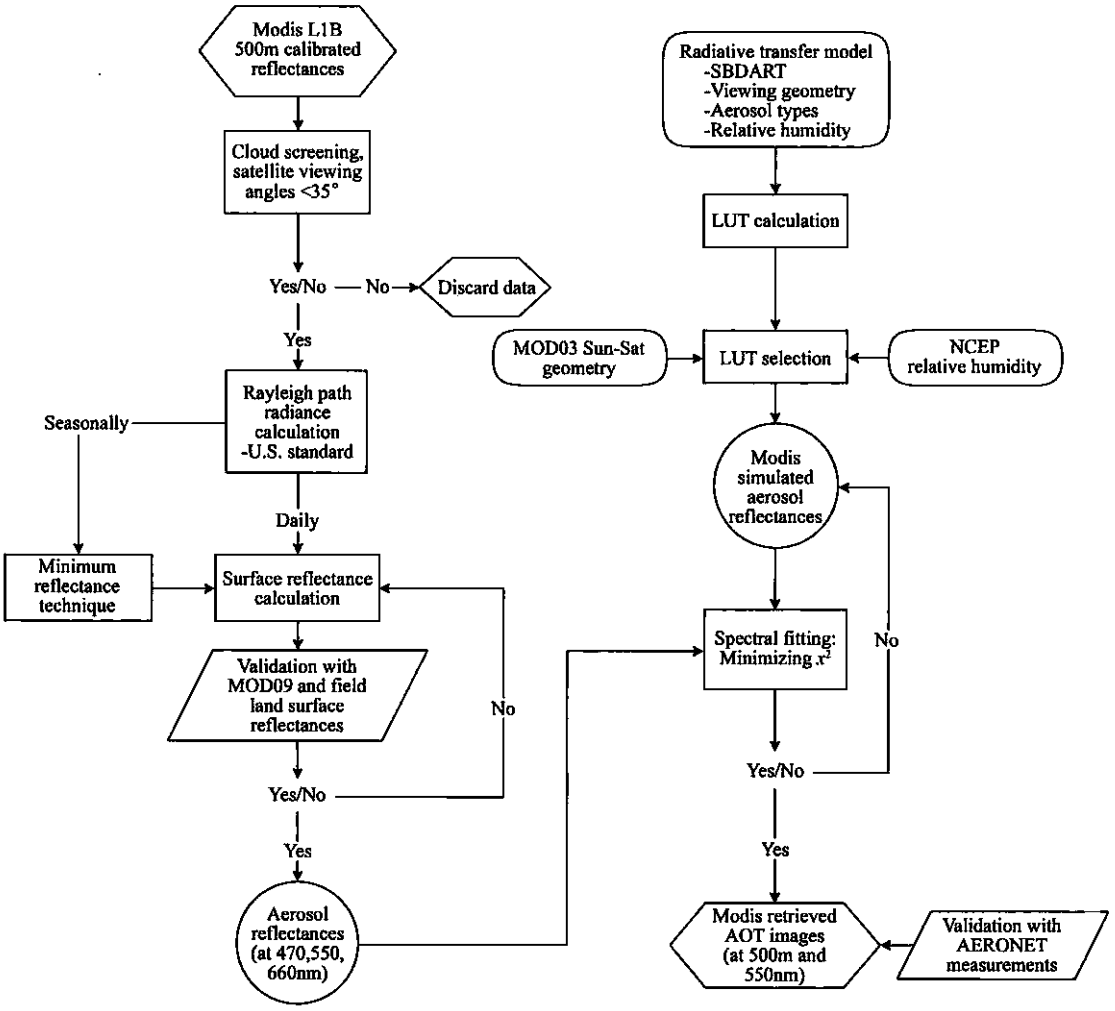

Figure 2. Schematic diagram for aerosol retrieval in the study

is the height. A Digital Elevation Model (DEM) in MOD03 geolocation data was used for estimating the height z and for calculating the pressure $p(z)$ for each pixel.

The basic scheme of the modified MRT is to extract the minimum reflectance values of land surfaces over a time period. To overcome the seasonal land cover changes, seasonal minimum reflectance images were derived based on at least thirty clear-sky images from each season. Then, the second minimum reflectance values were retrieved to prevent abnormal low reflectance such as noise or shadow. Comparisons were undertaken between minimum reflectance images and MODIS surface reflectance products (MOD09) and field surface measurements. The differences between minimum reflectance and MOD09 images are 3%, 1% and 1% at 470nm, 550nm and 660nm respectively, and the differences between minimum reflectance and MSR field measurements are 3%, 2% and 2% at 470nm, 550nm and 660nm respectively. It is noted that the second minimum reflectance values have a stronger agreement with the surface reflectances. In addition, cloud screening was used for determining cloud contamination which is important particularly in cloud-prone area like Hong Kong. Since there is no high resolution thermal band in MODHKM (500m) data, a tailor-made cloud-masking algorithm is proposed for this study by making use of three visible channels and an NDVI band. This algorithm tests the brightness of reflectance for each pixel, with thresholds set based on a trial-and-error approach (equation 4). The nadir images with satellite viewing angle <35° have only been considered in order to minimize the angular effects caused by bidirectional reflectivity in the heterogeneous areas.

If (reflectance at 470nm >0.2) or (reflectance at 550nm >0.2) or (reflectance at 660nm>0.2) or (NDVI < –0.5) then mask (4)

B. Aerosol retrieval

This study used the Santa Barbara DISORT Radiative Transfer (SBDART (Ricchiazzi, et al., 1998)) code for constructing the LUT, which is used to calculate the aerosol reflectance as a function of AOT under various sun-viewing geometries and relative humidity (RH). Input data for SBDART consists of three main types, namely atmosphere, aerosol, and surface data. A few aerosol models from the Optical Properties of Aerosols and Clouds (OPAC (Hess, et al., 1998)) database were used in this study. Each aerosol model is characterized by its own microphysical and optical properties, such as

particle size distribution, complex refractive indices, RH, etc. They are classified as i. continental clean (CC), ii. continental average (CA), iii. continental pollutant (CP), iv. desert dust (DD), v. maritime clean (MC), vi. marine pollutant (MP) models.

For the LUT construction, above 6 aerosol models with 9 solar zenith angles (0°–80°, Δ=10°), 17 view zenith angles (0°–80°, Δ=5°), 18 relative sun/satellite azimuth angles (0°–170°, Δ=10°), 8 RH values (RH=0%, 50%, 70%, 80%, 90%, 95%, 98%, and 99%) are considered. The SBDART code uses the aerosol properties associated with a given model, plus the combinations of values for the 5 parameters listed above (amounting to 132,192 combinations at 3 bands (470, 550, 660 nm)), to compute hypothetical AOT. Figure 3 represents one of the numerous LUTs from the SBDART results.

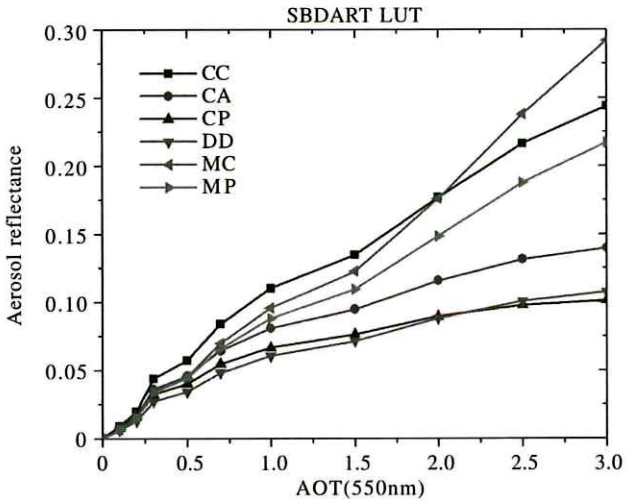

Figure 3. Aerosol reflectance as a function of AOT. The SBDART calculations were performed with solar zenith angle=30°, satellite zenith angle=10°, azimuth angle=150°, and RH=50%

The first step in this retrieval starts from reading of the LUTs with specific RH. RH values are acquired from the National Center for Environmental Prediction (NCEP) model (Kalnay et al., 1996). The second step is the interpolation of the LUT geometry to the measured (satellite) geometry. These two steps can reduce the number of LUT values being read in the computer memory. In the third step, hypothetical aerosol reflectances are determined based on the satellite estimated aerosol reflectance in the 470nm band. Finally, the satellite observed aerosol reflectances are compared to the set of hypothetical aerosol reflectances for each geometrically-corrected LUT. For these comparisons, an optimal spectral shape-fitting technique was executed for selecting the appropriate aerosol model with the smallest systematic errors (Kaufman and Tanré, 1998; Costa, et al., 1999; Torricella, et al., 1999; Lee, et al., 2007). The optimal spectral shape-fitting algorithm is expressed as:

$$x^2 = \frac{1}{n}\sum_{i=1}^{n}\left(\frac{\rho^m_{\text{Aer}}(\lambda_i)-\rho^a_{\text{Aer}}(\lambda_i)}{\rho^m_{\text{Aer}}(\lambda_i)}\right)^2 \quad (5)$$

where the error term of x^2 is described as the residual of the measured aerosol reflectances $\rho^m_{\text{Aer}}(\lambda_i)$ from MODIS and modelled aerosol reflectances $\rho^a_{\text{Aer}}(\lambda_i)$ from aerosol models. The minimum residual of x^2 is selected among six aerosol types for each pixel. Thus, the appropriate aerosol type is selected and the corresponding AOT values are then derived for each pixel.

IV. RESULTS

Validation with AERONET measurements

To evaluate the performance of our methodology, the MODIS 500m retrieved AOT was validated with the AERONET measurements for 2007 (Figure 4(a)). The MOD04 collection 4 and 5 AOT data were also compared with the AERONET (Figure 4(b)). Good agreements are shown between the MODIS 500m AOT and AERONET, with a linear-fitting correlation coefficient (r) of 0.937, which is higher than those from MOD04 collection

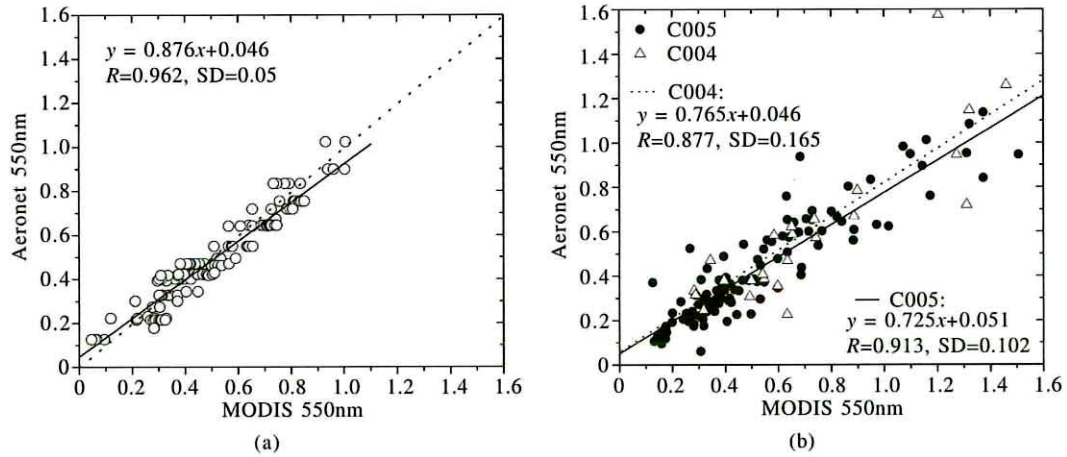

Figure 4. Comparison plot, a. between MODIS 500m AOT with AERONET measurements; b. between MOD04 collection 4 and 5 AOT with AERONET measurements. Note that there is insufficient of MOD04 collection 4 data in the NASA GSFC database since the collection 4 data is replaced with collection 5 data in schedule, only twenty-four measurements were temporarily matched with AERONET data

5 (r = 0.913) and MOD04 collection 4 (r = 0.877) data. In addition, the slope of the linear-fitting equation on the MODIS 500m plot (Figure 4(a)) is closer to unity and thus performs better than those for collection 4 and 5 (Figure 4(b)). Although a strong correlation is revealed between MODIS 500m AOT and AERONET data, it tends to underestimate the AOT by approximately ~0.046. Similar values (~0.046 and 0.051) are also shown for the collection 4 and collection 5 data. Most importantly, our methodology can retrieve AOT images at a detailed level and can retrieve AOT over both urban and vegetated areas. This is a significant improvement for AOT retrieval in areas of complex topography such as Hong Kong.

The AOT distribution over Hong Kong and the PRD region on 20 October 2007 retrieved using MODIS 500m data, with a resolution of 500m × 500m is shown in Figure 5(b). The AOT is relatively high ranging between ~0.6 in rural areas to ~1.6 in urban. It is noted that the AOT values are high in urban areas due to anthropogenic pollution but are comparative small in the countryside. The northern part of Hong Kong especially nearly the border of Shenzhen has long suffered from cross-boundary pollutants emitted from industries in the PRD region, and high AOT values of 1.0 are observed. In Figure 5(b), severe air pollution was observed in the Guangzhou area, which is caused by industries and power plant emissions. The pollutants are often trapped in the PRD region due to low wind speeds (~2ms^{-1}) in the autumn. In contrast, results from the MODIS collection 5 algorithm with coarser resolution (10km × 10km) (Figure 5(a)) compares less favorably, and is ineffectual for aerosol mapping in spatially detailed, complex, and Vrbanized regions.

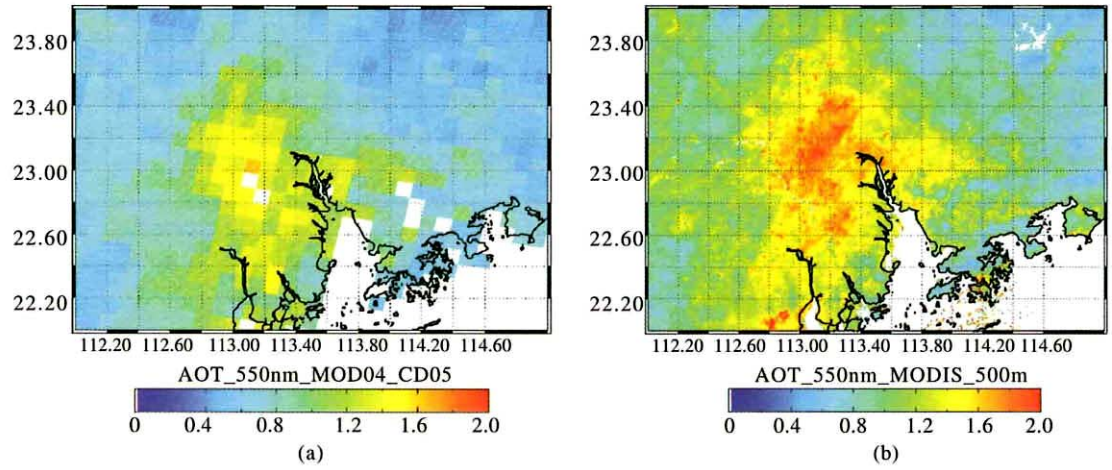

Figure 5. (a) AOT at 550nm derived from MODIS MOD04 collection 5 algorithm and (b) from this study with 500 × 500m^2 over Hong Kong over the Pearl River Delta (PRD) region

V. CONCLUSION

A new aerosol retrieval algorithm for MODIS 500m data which is able to estimate aerosols at a detailed level over both urban and rural areas was proposed in this study. This method is coupled with the modified MRT to derive surface reflectance images as well as with comprehensive LUTs which consider the various aerosol models, sun-satellite geometries and RH conditions in radiative transfer modeling. The derived MODIS 500m AOT showed good accuracy (r=0.962) compared with ground-based AERONET measurement, and lower correlations were found for MODIS collection 5 (r=0.913) and collection 4 (r=0.877) data. The higher accuracy and higher spatial resolution obtained from the MODIS 500m AOT images permits their use for study of cross-boundary transient aerosols and local anthropogenic aerosol loading distributions.

ACKNOWLEDGEMENTS

The authors wish to acknowledge the NASA Goddard Earth Science Distributed Active Archive Center for the MODIS Level IB and Level 2 data, the NOAA for the NCEP model, and Brent Holben for help with the Hong Kong PolyU AERONET station. Grant PolyU5253/U7E supported this research.

REFERENCES

[1] Kaufman, Y. J., D. Tanré, 1998, Algorithm for remote sensing of tropospheric aerosol from MODIS. NASA MOD04 product ATBD report.

[2] Chu, A., Y. J. Kaufman, C. Ichoku, L. A. Remer, D. Tanré, and B. N. Holben, 2002, Validation of MODIS aerosol optical depth retrieval over land. Geophysical Research Letters, 29(12):1–4.

[3] Holben, B. N., T. F. Eck, I. Slutsker, D. Tanre, J. P. Buis, A. Setzer, E. F. Vermote, J. A. Reagan, Y. J. Kaufman, T. Nakajima, F. Lavenu, I. Jankowiak, A. Smirnov, 1998, AERONET-A federated instrument network and data archive for aerosol characterization. Remote Sensing of Environment, 66(1):1–16.

[4] Remer, L. A., Y. J. Kaufman, D. Tanré, S. Mattoo, D. A. Chu, J. V. Martins, R. R. Li, C. Ichoku, R. C. Levy, R. G. Kleidman, T. F. Eck, E. Vermote, B. N. Holben, 2005, The MODIS Aerosol Algorithm, Products and Validation. Journal of the Atmospheric Sciences, 62(4):947–973.

[5] Levy, R. C., L. A. Remer, J. V. Martins, Y. J. Kaufman, A. Plana-

fattori, J. Redemann, B. Wenny B., 2004, Evaluation of the MODIS aerosol retrievals over ocean and land during CLAMS. Journal of the Atmospheric Sciences, 62(4):974–992.

[6] Levy, R. C., L. A. Remer, S. Mattoo, E. F. Vermote, Y. J. Kaufman, 2007, Second-generation operational algorithm: Retrieval of aerosol properties over land from inversion of Moderate Resolution Imaging Spectroradiometer spectral reflectance. Journal of Geophysical Research, 112, D13211.

[7] Mi, W., Z. Q. Li, X.G. Xia, B. Holben, R. Levy, F. S. Zhao, H. B. Chen, M. Cribb, 2007, Evaluation of the MODIS Aerosol Products at Two AERONET Stations in China. Journal of Geophysical Research, 112, D22S08.

[8] Li, Z., F. Niu, K. H. Lee, J. Xin, W. M. Hao, B. Nordgren, Y. Wang, P. Wang, 2007, Validation and Understanding of MODIS Aerosol Products Using Ground-based Measurements from the Handheld Sunphotometer Network in China. Journal of Geophysical Research, 112, D22S07.

[9] Hsu, N. C., S. C. Tsay, M. D. King, J. R. Herman, 2004, Aerosol Properties Over Bright Reflecting Source Regions. IEEE Transaction of Geoscience and Remote Sensing, 42(3):557–569.

[10] Hsu, N. C., S. C. Tsay, M. D. King, J. R. Herman, 2006, Deep Blue Retrievals of Asian Aerosol Properties During ACE-Asia. IEEE Transaction of Geoscience and Remote Sensing, 44(11): 3180–3195.

[11] Herman, J. R., E. A. Celarier, 1997, Earth surface reflectivity climatology at 340–380 nm from TOMS data. Journal of Geophysical Research, 102: 28003–28011.

[12] Koelemeijer, R. B. A., J. F. de Haan, P. Stammes, 2003, A database of spectral surface reflectivity in the range 335–772 nm derived from 5.5 years of GOME observations. Journal of Geophysical Research, 108: 28003–28011.

[13] Li, C. C., A. K. H. Lau, J. T. Mao, D. A. Chu, 2005, Retrieval, validation, and application of the 1-km aerosol optical depth from MODIS measurements over Hong Kong. IEEE Transaction of Geoscience and Remote Sensing, 43(11): 2650–2658.

[14] Bucholtz, A., 1995, Rayleigh-scattering calculations for the terrestrial atmosphere. Applied Optics, 34: 2765–2773.

[15] Ricchiazzi, P., S. R. Yang, C. Gautier, D. Sowle, 1998, SBDART: A research and teaching software tool for plane-parallel radiative transfer in the Earth's atmosphere. Bulletin of the American Meteorological Society, 79(10): 2101–2114.

[16] Hess, M., P. Koepke, I. Schult, 1998, Optical Properties of Aerosols and clouds: The software package OPAC. Bulletin of the American Meteorological Society, 79: 831–844.

[17] Kalnay, E., M. Kanamitsu, R. Kistler, W. Collins, D. Deaven, L. Gandin, M. Iredell, S. Saha, G. White, J. Woollen, Y. Zhu, A. Leetmaa,B. Reynolds, M. Chelliah, W. Ebisuzaki, W. Higgins, J. Janowiak, K. C. Mo, C. Ropelewski, J. Wang, R. Jenne, D. Joseph, 1996, The NCEP/NCAR 40-year reanalysis project. Bulletin of the American Meteorological Society, 77(3): 437–470.

[18] Costa, M. J., M. Cervino, E. Cattani, F. Torricella, V. Levizzani, A. M. Silva, 1999, Aerosol optical thickness and classification: Use of METEOSAT, GOME and modeled data. EOS-SPIE International Symposium on Remote Sensing, Proc. SPIE Vol. 3867, Satellite Remote Sensing of Clouds and the Atmosphere IV, J. E. Russell (Ed.), pp.268–279.

[19] Torricella, F., E. Cattani, M. Cervino, R. Guzzi, C. Levoni, 1999, Retrieval of aerosol properties over the ocean using global ozone monitoring experiment measurements: Method and applications to test cases. Journal of Geophysical Research, 104(D10): 12085–12098.

[20] Lee, K. H., Y. J. Kim, W. von Hoyningen-Huene, J. P. Burrow, 2007, Spatio-Temporal Variability of Atmospheric Aerosol from MODIS data over Northeast Asia in 2004. Atmospheric Environment, 41(19): 3959–3973.